Reaction of gaseous mercury with molecular iodine, atomic iodine, and iodine oxide radicals — Kinetics, product studies, and atmospheric implications

Farhad Raofie, Graydon Snider, and Parisa A. Ariya

Abstract: Mercury is present in the Earth's atmosphere mainly in elemental form. The chemical transformation of mercury in the atmosphere may influence its bioaccumulation in the human food chain as well as its global cycling. We carried out the first kinetic and product studies of the reactions of gaseous mercury with molecular iodine, atomic iodine, and iodine oxide radicals at tropospheric pressure (~740 Torr) and 296 ± 2 K in air and in N_2 (1 Torr = 133.322 4 Pa; 0 °C = 273.15 K). Atomic iodine was formed using UV photolysis of CH_2I_2. IO radicals were formed by the UV photolysis of CH_2I_2 in the presence of ozone The reaction kinetics were studied using absolute rate techniques with gas chromatographic and mass spectroscopic detection (GC–MS). The measured rate coefficient for the reaction of Hg^0 with I_2 was $\leq (1.27 \pm 0.58) \times 10^{-19}$ cm^3 molecule^{-1} s^{-1}. The reaction products were analyzed in the gas phase from the suspended aerosols and from deposits on the walls of the reaction chambers using six complementary methods involving chemical ionization and electron impact mass spectrometry, GC–MS, a MALDI-TOF mass spectrometer, a cold vapor atomic fluorescence spectrometer (CVAFS), and a high-resolution transmission electron microscope (HRTEM) coupled to an energy dispersive spectrometer (EDS). The major reaction products identified were HgI_2, HgO, and HgIO or HgOI. The implications of the results are discussed with regards to both the chemistry of atmospheric mercury and its potential implications in the biogeochemical cycling of mercury.

Key words: mercury, molecular iodine, atomic iodine, iodine oxide radicals kinetics, product study, atmospheric chemistry.

Résumé : Dans l'atmosphère terrestre, le mercure est principalement présent sous la forme élémentaire. La transformation chimique du mercure dans l'atmosphère peut influencer sa bioaccumulation dans la chaîne alimentaire de l'homme ainsi que sur son cycle global. On a effectué les premières mesures cinétiques ainsi que les premières études sur la nature des produits des réactions du mercure gazeux avec l'ion moléculaire, l'iode atomique et les radicaux d'oxyde d'iode, à la pression de la troposphère (environ 740 Torr, 1 Torr = 133.322 4 Pa), à 296 ± 2 K, dans l'air et dans l'azote. L'iode atomique a été obtenu par photolyse UV du CH_2I_2. Les radicaux IO ont été formés par la photolyse UV du CH_2I_2 en présence d'ozone. On a étudié la cinétique des réactions par les techniques de vitesses absolues en utilisant une combinaison des techniques de la chromatographie en phase gazeuse et de la spectrométrie de masse (CG-SM). La valeur du coefficient de vitesse mesuré pour la réaction du Hg^0 avec le I_2 est inférieure à $(1{,}27 \pm 0{,}58) \times 10^{-19}$ cm^3 molécule^{-1} s^{-1}. Les produits de la réaction ont été analysés par chromatographie gazeuse, à partir d'aérosols en suspension ainsi qu'à partir des dépôts recueillis des parois des chambres réactionnelles en faisant appel à six techniques complémentaires impliquant la spectrométrie de masse avec ionisation chimique ainsi que l'ionisation avec impact électronique, la CG-SM et la spectrométrie de masse à temps d'envol avec ionisation par désorption au laser assistée par une matrice (IDLAM), un spectromètre à fluorescence atomique avec vapeur froide (SFAVF) et un microscope à transmission d'électron à haute résolution (MTEHR) couplé à un spectromètre à dispersion d'énergie (SDE). Les produits principaux qui ont pu être identifiés sont le HgI_2, le HgO et le HgIO ou HgOI. On discute des implications de ces résultats en regard tant de la chimie du mercure atmosphérique que de ses implications potentielles dans le cycle biogéochimique du mercure.

Mots-clés : mercure, iode moléculaire, iode atomique, radicaux d'oxyde d'iode, cinétique, étude de produits, chimie de l'atmosphère.

[Traduit par la Rédaction]

Received 19 December 2007. Accepted 25 April 2008. Published on the NRC Research Press Web site at canjchem.nrc.ca on 5 July 2008.

F. Raofie, G. Snider, and P.A. Ariya.[1] Departments of Chemistry and Atmospheric and Oceanic Sciences, McGill University, 801 Sherbrooke St. W., Montreal, QC H3A 2K6, Canada.

[1]Corresponding author (e-mail: parisa.ariya@mcgill.ca).

 doi:10.1139/V08-088

Introduction

Gaseous elemental mercury is a toxic element of concern because of its accumulation in the aquatic food chain (via methylation), leading to mercury deposits found in consumable freshwater and marine species (1). Mercury is released into the atmosphere from a variety of natural (2–6) and anthropogenic sources (7–10). It has been shown that 60% to 80% of present mercury emissions into the atmosphere are of anthropogenic origin, and that about 50% of anthropogenic mercury emissions enter a global cycle of contamination (11). The concentration of atmospheric mercury in the northern hemisphere is between 1.6 to 4.7 ng m^{-3}, with an average of 2.5 ng m^{-3}, which is mainly elemental (12). Atmospheric mercury undergoes various chemical and physical transformations before being deposited on the ground. Unexpectedly rapid depletion of elemental mercury has been observed in the high Arctic (13), Arctic (14, 15), and sub Arctic (16) during springtime, concomitant with ozone depletion. It has been shown that chain reactions of halogen species in the Arctic are responsible for ozone and mercury depletion (17–21). The speciation and chemical transformations of mercury in the atmosphere strongly influence its deposition and global cycling. Hg^0 can be transported back to the earth mainly through dry deposition. Mercury(II) oxides are nonvolatile species and precipitate to the ground much more rapidly than Hg^0 via dry and wet processes (22).

Experimental and theoretical research of gas-phase reactions of mercury with halogen species under atmospheric conditions are relatively new, most of which have only been published within the last decade. Schroeder et al. (23) proposed several possible reactions between gaseous mercury and a variety of atmospheric oxidants and reductants using their thermodynamic data. They suggest that O_3 and Cl_2 may be important for oxidation of Hg^0, while SO_2 and CO are important for the reduction of Hg(II). It has since been found that bromine species play an important role in the rapid Arctic depletion of mercury. In warmer climates, however, oxidation by ozone becomes the most relevant pathway. In our laboratory, we have studied products of the gas-phase reaction of elemental mercury with O_3 (24), BrO (25, 26), and HO (27) radicals; atomic Cl and Br; and molecular Cl_2 and Br_2 (28). We have also considered previous thermochemical calculations of reactions between Hg and halogens (29).

The atmospheric chemistry of iodine is important for several reasons, including the influence of iodine oxides on the oxidizing capacity of the troposphere, the formation of new particles, the enrichment of iodine in marine aerosols, and transport of this essential dietary element to the continents (30). The identified natural sources of iodine are CH_3I, CH_2I_2, C_2H_5I, CH_2ICl, and I_2 from seawater (31–33) that photochemically can release reactive iodine species. Iodine, however, is also released into the atmosphere from industrial activity. The photolysis of many iodine species produces iodine atoms, and hence IO radicals through reaction with O_3 (34). Iodine oxide was observed in the marine boundary layer by several researchers (35, 36). The iodine oxide radicals are involved in ozone depleting cycles in the troposphere (33, 37) and stratosphere (38) as well as reaction with dimethyl sulfide emitted by phytoplankton in the ocean (39). However, there is no available literature on the experimental kinetic and product of molecular iodine, atomic iodine, and iodine oxide radicals with elemental mercury (see Calvert and Lindberg for simulations of iodine kinetics (40)).

The purpose of this work is to study the products of the gas-phase reaction of elemental mercury with molecular iodine, atomic iodine, and iodine oxide radicals and kinetics of the gas-phase reaction of elemental mercury with molecular iodine at tropospheric pressures and ambient temperatures.

Experimental section

Experimental procedure

Experiments were carried out in N_2 and in air at room temperature and near-atmospheric pressure. Reaction chambers included 1 to 50 L Teflon bags and 1 to 5 L Pyrex double-wall flasks equipped with magnetic stirrers to assure homogeneous mixing. The reaction chamber temperature was maintained at 296 ± 2 K (0 °C = 273.15 K) by circulating water through the outer jacket using a Neslab RTE 111 circulator.The reaction chamber was washed a minimum of four times with concentrated nitric acid (12 mol/L), Mili-Q water, and acetone and dried at high temperature (398 K) overnight. The inside walls of the reaction flask were coated with halocarbon wax (Supelco) to prevent unwanted wall reactions (41). A vacuum system was used to prepare gaseous reactant mixtures. Gaseous reactants were transferred directly into the reaction mixture using a 10 or 250 μL syringe (Hamilton series 1800 gas tight). Liquid substrates were injected with a 2 or 10 μL syringe (Hamilton series 700). Ozone was produced using an ozone generator (Model OL 100/DS, Ozone Services Inc.) by a silent discharge technique and was trapped on silica gel cooled to 200 K in a dry ice – acetone mixture. Ozone was then transferred to an evacuated flask (~10^{-7} bar) (1 bar = 100 kPa), and the concentration of ozone was monitored by a UV–vis spectrometer (Varian Cary-50-Bio). A given amount of ozone was injected into the reaction flask (1 to 5 L) using a gas-tight syringe. Molecular iodine vapor was produced by mixing iodine with silica gel and heating to 323 K. Iodine radicals were generated in situ upon UV photolysis of diiodomethane ($300 \leq \lambda \leq 400$ nm).

IO radicals were generated in situ upon UV photolysis of diiodomethane ($300 \leq \lambda \leq 400$ nm) in the presence of ozone (42).

[R1] $CH_2I_2 + h\upsilon\ (300 \leq \lambda \leq 400\ nm) \rightarrow CH_2I^{\cdot} + I^{\cdot}$

[R2] $I^{\cdot} + O_3 \rightarrow IO + O_2$

$$k_{R2} = 8 \times 10^{-13}\ cm^3\ molecule^{-1}\ s^{-1}$$

The initial concentration of Hg^0 was ~0.5 ppm, and the concentration of I_2 was 130 ppm. In the course of ozone addition, we used scavengers such as trimethyl benezene for OH radicals (41) that are formed via side reactions in the presence of organic matter, such as CH_2I_2 or any undesired impurities or production of other undesired oxidants in the course of experiments. We did not observe any organomercury or halo-organo-mercury products using six different analytical methods. The reaction of gaseous mercury with O_3 is too slow [$(6.2 \pm 1.1) \times 10^{-19}$ cm^3 $molecule^{-1}s^{-1}$ (43)]

to observe. Oxidation of gaseous mercury by O_3 was negligible under the reaction conditions.

Analytical procedure for the product analysis

The reactions

[R3] $Hg^0_{(g)} + I_{2\,(g)} \rightarrow$ products

[R4] $Hg^0_{(g)} + I_{(g)} \rightarrow$ products

and

[R5] $Hg + IO^{\cdot}_{(g)} \rightarrow$ products

were carried out in 1 to 50 L Teflon bags and 1 to 5 L Pyrex flasks. The products were analyzed by the methods described below.

Direct mass spectrometry

Reaction products were collected using two methods. In the first method, the reaction products were passed through a 1.1 mm i.d. × 10 cm length Pyrex tube (Corning) immersed in liquid nitrogen. In the second method, the walls of the reaction flask were washed with concentrated HCl. A sample of the collected products (50 μL) was transferred in a 1.1 i.d. × 10 cm length Pyrex tube and was covered immediately with a piece of glass wool. Extra HCl was evaporated by slow heating in a water bath. Finally, the collected products in the tube were evaporated at stepwise elevated temperatures to the chemical and electron impact ion source of a Kratos MS25RFA mass spectrometer.

Cold vapor atomic fluorescence spectrometry (CVAFS)

Samples were prepared by washing the walls of the reaction chamber, a Teflon filter (0.45 μm), and the coiled Pyrex trap, with a mixture of 20 mL HNO_3 and 0.5 mL 30% H_2O_2, diluted to 50 mL with Milli-Q water. The samples were heated to 350 K for 1 h to decompose excess H_2O_2, diluted further to 100 mL in a volumetric flask with Milli-Q water, and analyzed using a cold vapor atomic fluorescence spectrometer (Tekran 2600).

Derivatization

This method is based on chemical transformation of Hg^{2+} to $HgCl_2$ and then to a more volatile organomercury compound, n-Bu_2Hg. Samples were prepared by washing the walls of the reaction flask with HCl, which transformed Hg^{2+} to $HgCl_2$. The sample was heated to remove extra HCl, which resulted in the formation of a white residue. Derivatization was performed using previously reported method (44, 45). 2 mL of toluene and 0.4 mL of 2 mol/L n-butylmagnesium chloride in tetrahydrofuran were added to the white residue. The mixture was then centrifuged at 0 °C for 10 min with occasional shaking. To quench the excess derivatizing agent, 0.4 mL of 0.6 mol/L HCl was added the mixture that was then centrifuged, allowing for collection of the organic phase for analysis.

[R6] $Hg^{2+} + 2\ HCl \rightarrow HgCl_2 + 2H^+$

[R7] $HgCl_2 + 2\ n\text{-}BuMgCl \rightarrow n\text{-}Bu_2Hg + 2MgCl_2$

Fig. 1. Typical absolute-rate data for reaction of Hg + I_2, [Hg] = 0.5 ppm, [I_2] = 3.2×10^{15} molecule cm^{-3}; kinetic runs were performed at 298 K in nitrogen.

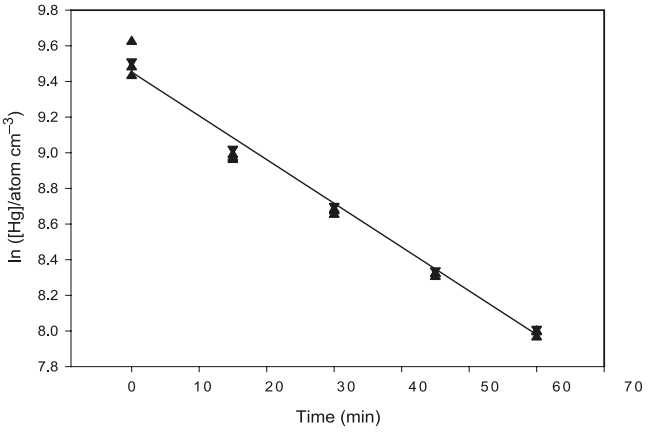

Transmission electron microscopy (TEM)

Reaction products were collected by two different methods. The first technique involved placing carbon-coated Cu grids on the surface of the reaction flask, and the Cu grids were later collected upon completion of the reaction. The second method involved the collection of reaction products in a capillary Pyrex tube, which was immersed in liquid nitrogen. Collected products were analyzed using a high-resolution transmission electron microscope (JEOL 2000 FX TEM). The elemental composition was qualitatively determined by energy dispersive spectroscopy (EDS; JEOL 2000).

Matrix-assisted laser desorption ionization time-of-flight mass spectrometry (MALDI-TOF-MS)

The reaction products were collected in capillary Pyrex tubes, which were immersed in liquid nitrogen. The collected products were analyzed using Kratos Kompakt MALDI-TOF-MS in reflectron mode. Dithranol and lithium bromide were used as matrix and cationization agent, respectively. The matrix has resonance absorption at laser wavelength of 337 nm. This rapid heating results in expulsion and soft ionization of the sample molecules without major fragmentation (46).

Chemicals and materials

Mercury (99.99% purity) and n-butyl magnesium chloride (2 mol/L solution in tetrahydrofuran) were supplied by Sigma-Aldrich. Nitrogen (99.998%), argon (99.999%), helium (99.999%), nitric oxide (99.99%), and extra-dry oxygen were obtained from Matheson. Toluene (99.9%), hydrogen peroxide (30%), hydrochloric acid (trace-metal grade), Iodine (99.9%), and nitric acid (trace-metal grade) were purchased from Fisher. Tin (II) chloride (99.999%) and diiodomethane (99%) were obtained from Aldrich. Milli-Q water of 18.2 MΩ cm resistivity was used for all experiments. The nitric and hydrochloric acids used in the course of experiments were 70 wt% and 38 wt% assays, respectively.

Fig. 2. Mass spectra of products formed in the reaction of Hg^0 with molecular iodine.

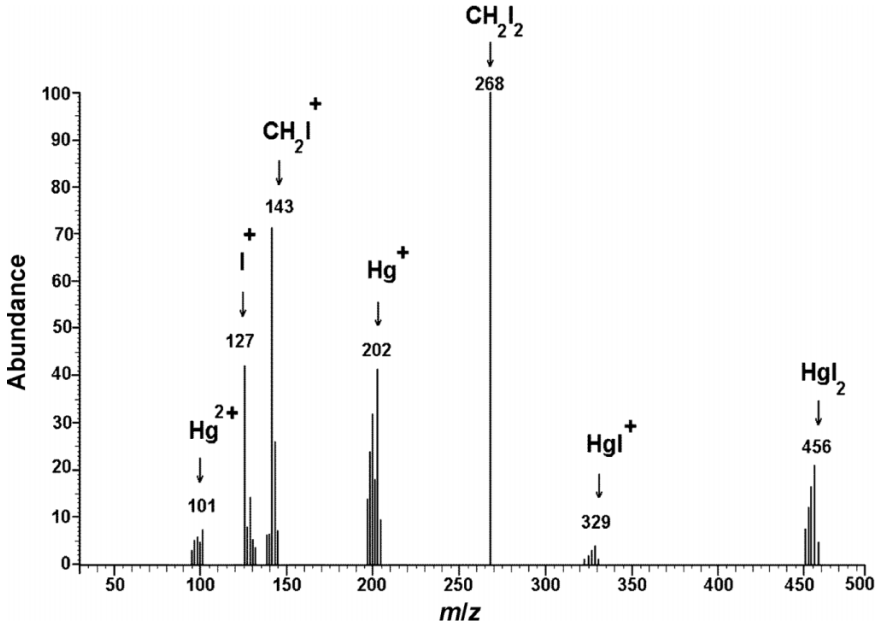

Fig. 3. Mass spectra of products formed in the reaction of Hg^0 with IO radicals.

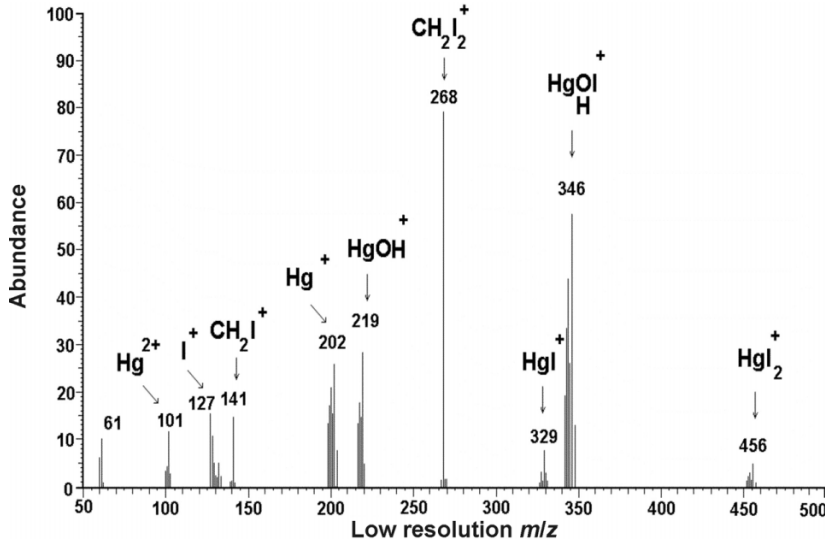

Results and discussion

Kinetic study

The absolute-rate technique was used to study the kinetics of the I_2-initiated reaction of Hg^0 (47). Experiments were carried out in 1 to 5 L Pyrex flask at room temperature in air and nitrogen. To prevent wall reaction, the walls of reaction flask were coated with halocarbon wax. In addition, to minimize the effect of adsorption on the kinetic results, the reaction mixture was kept at equilibration for 2 h before injecting I_2. To inject I_2 as a gas into the reaction chamber, molecular I_2 was first mixed with silica gel (~ 1:50) in 1 L flask. The mixture was evacuated to 7×10^{-3} Torr. The temperature of the flask was increased to 60 °C by slow heating. A given amount of I_2 was injected into the reaction chamber using gas-tight syringe. To prevent dissociation of I_2, the reaction chamber was completely dark. The reaction of gaseous mercury with I_2 was studied under pseudo first-order conditions by monitoring the MS signal of mercury vs. time. Figure 1 shows semi logarithmic plots of data obtained for the reaction of Hg^0 with I_2 in air. The upper-limit rate coefficient calculated from the curve was $\leq (1.27 \pm 0.58) \times 10^{-19}$ cm^3 $molecule^{-1}s^{-1}$. Because we observed the formation of particulate matter, we cannot rule out the possibility of heterogeneous reactions; and hence, this rate coefficient value should represent only an upper limit for the gas-phase-initiated oxidation of elemental mercury with iodine molecule.

Product studies

The products of reactions [R3–R5] have been studied in the gas phase from suspended aerosols and from the walls of

Fig. 4. Mass spectra of $HgCl_2$ and HgI_2, reaction products in reaction of Hg^0 with atomic iodine.

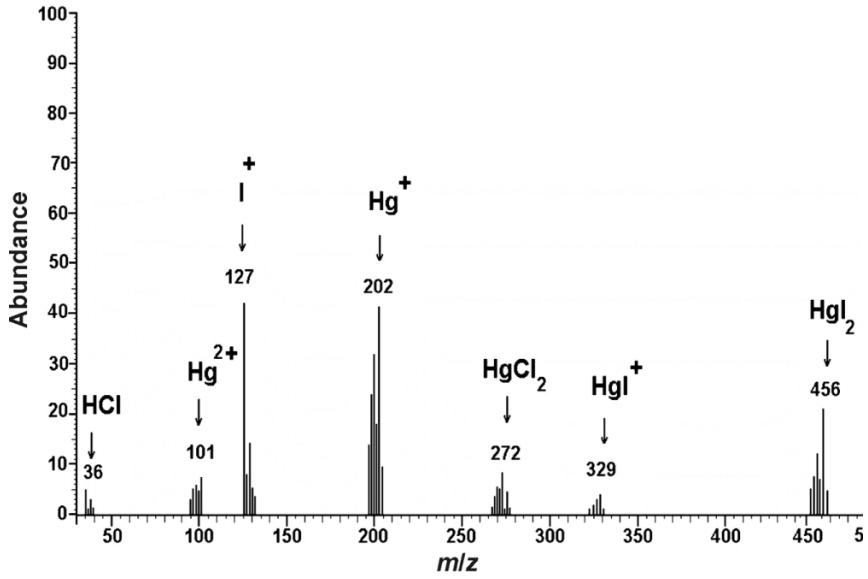

the reaction chambers. Six complementary analytical methods have been employed to identify the reaction products of molecular iodine, atomic iodine, and iodine radicals initiated oxidation of $Hg^0_{(g)}$.

In the first method, after the reaction was completed, the reaction products from the gas–aerosol phase were collected in a liquid-nitrogen-cooled capillary tube. The chemical structure of the reaction products mixture was identified using a direct MS instrument equipped with an electron impact and chemical ionization ion source with probe temperature elevated to 430 K. Figure 2 represents mass spectra of HgI_2. The isotopic ratios for HgI_2 (33.6:56.4:77.5:44.3:100.0:22.8) corresponded well with the anticipated *m*/*z* ratios 452, 453, 454, 455, 456, and 458, respectively; thus further supporting the identified mercury compounds. The *m*/*z* ratio of 268 is assigned to CH_2I_2, which had been used as the iodine radical source. Other *m*/*z* ratios in the mass spectrum represent the fragmentation of HgI_2 or CH_2I_2. Hence, our results identify HgI_2 as the major product of the gas–aerosol reaction: Hg^0 + I_2. For Hg^0 + I˙, the same product was observed. For Hg^0 + IO˙, chemical ionization of NH_3 was used as an ion source, so the observed mass spectra of the ion (M^+) should be increased by one. We identified the products HgOI or HgIO, HgI_2, and HgO (Fig. 3). The *m*/*z* ratio of each peak was shifted by one. Moreover, the observed isotopic ratios for HgI_2 (33.6:56.4:77.5:44.3:100.0:22.8) corresponded well with the anticipated *m*/*z* ratios of 452, 453, 454, 455, 456, and 458, respectively. The isotopic ratios of 33.5, 56.3, 77.5, 44.4, 100.0, and 23.0 correspond well with those for the *m*/*z* ratios 341, 342, 343, 344, 345, and 347, respectively. The isotopic ratios 33.5:56.3:77.4:44.4:100.0:23.0 matched *m*/*z* ratios of 214, 215, 216, 217, 218, and 220, repectively, illustrating the presence of HgO, which further supports the identified mercury compounds. The *m*/*z* ratio of 268 is assigned to CH_2I_2, which had been used as an iodine radical source. From product analysis, we were unable to distinguish the chemical structure of Hg-, I-, and O-containing species. Other *m*/*z* ratios in the mass spectrum represent either fragmentation of HgI_2, HgO, HgIO (HgOI), or CH_2I_2 in the ion source of the mass spectrometer. The results show that the major products in the gas–aerosol phase of reaction $Hg^0_{(g)}$ + IO˙ are HgIO or HgOI, HgI_2, and HgO.

In the second method, the walls of the reaction flask were washed with concentrated HCl. Samples of the collected products (50 μL) were transferred in a 1.1 i.d. × 10 cm length Pyrex tube and immediately covered with a piece of glass wool. Extra HCl was evaporated by slow heating in a water bath. Finally, the collected products in the tube were evaporated at stepwise elevated temperatures to the chemical and electron impact ion source of a Kratos MS25RFA mass spectrometer. Figure 4 represents the mass spectra of $HgCl_2$ and HgI_2. The isotopic ratios for $HgCl_2$ (22:37:65:52:100:22:62:16) corresponded well with the anticipated *m*/*z* ratios of 268, 269, 270, 271, 272, 273, 274, and 276, respectively. The *m*/*z* ratio of 456 is assigned to HgI_2, which is slightly soluble in concentrated HCl. Hence, we conclude the existence of HgI_2 as a reaction product on the walls. Similar results were observed for the Hg^0 + I˙ and Hg^0 + IO˙ reactions.

In the third method, to confirm the presence of Hg^{2+} on the walls of the reaction chamber, the products on the walls were converted to di(*n*-butyl mercury). The derivatized sample was analyzed using GC–MS. Figure 5 illustrates a chromatogram and mass spectrum of the derivatized mercury. Hg^0 and Hg^{+1} were not targeted in derivatization analysis, so their existence cannot be evaluated using the Grignard reagent. This experiment confirmed the presence of Hg^{2+} (here, HgI_2) on the walls of reaction chamber. Similar results were observed for the Hg^0 + I˙ and Hg^0 + IO˙ reactions.

In the fourth method, MALDI-TOF-MS was used to identify the reaction products of molecular iodine, atomic iodine, and iodine oxide radicals. Figure 6 is an example of a MALDI-TOF-MS spectrum. The peak at mass 454 is assigned to HgI_2 in the reaction of Hg with both I_2 and I. No other oxidized forms of mercury were detected. Figure 7 is an example of MALDI-TOF-MS spectrum for the reaction

Fig. 5. Gas chromatogram and the corresponding mass spectrum of the derivatized mercury (di-*n*-butylmercury) eluted at 12.25 min.

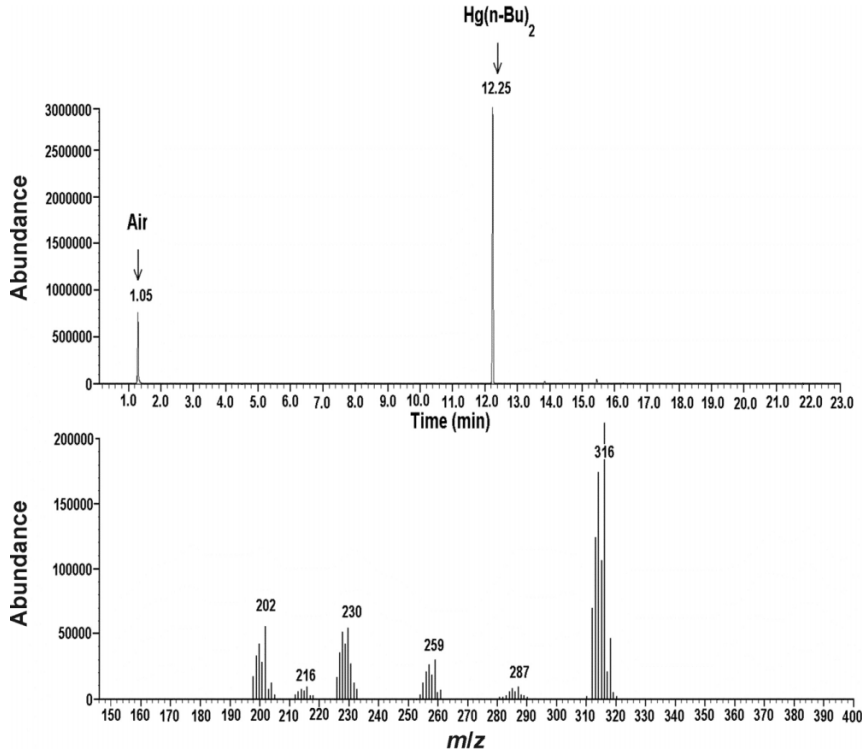

Fig. 6. MALDI-TOF mass spectrum of products formed in the reaction of Hg^0 with molecular iodine.

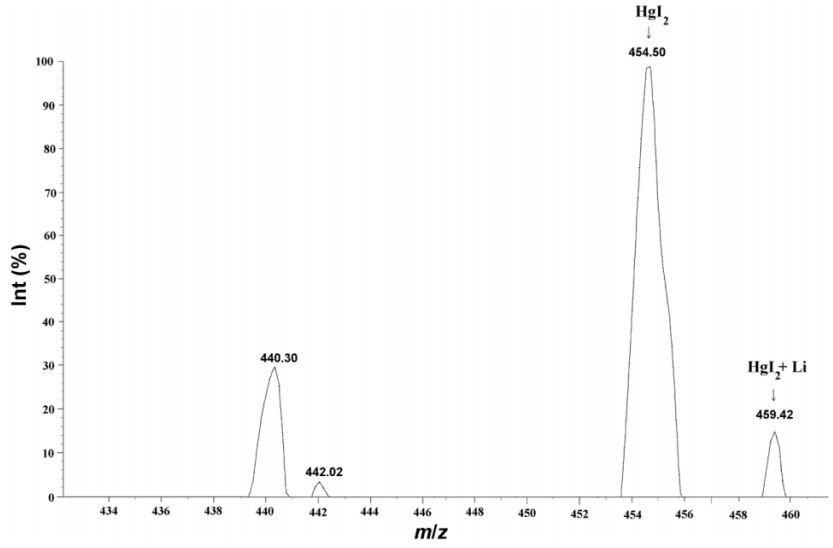

of Hg^0 + IO˙. The peak at mass 357 is assigned to HgIO or HgOI. Other peaks arise from the matrix itself under our experimental conditions.

In the fifth method, we attempted to identify the shape, size, and elemental composition of reaction products from the gas–aerosol phase and on the walls of the reaction chamber using HRTEM coupled to an EDS detector. Figure 8*a* illustrates the TEM image of air-dried products of the reaction Hg^0 + I_2 collected from the gas–aerosol mixture. The size of the particles in the gas–aerosol mixture was approximately 0.2 μm. The EDS spectrum of the chemical composition of the products in the gas–aerosol mixture showed that the gas–aerosol mixture should contain mercury and iodine. Combining evidence from MALDI-TOF-MS and EDS, we believe that the observed aerosol contains HgI_2. Figure 8*b* depicts TEM image of collected products of the reaction of Hg^0 + I_2 from the walls of the reaction chamber. The size and chemical composition of the particles collected from the walls of the reaction chamber exhibit similar features to those observed from gas–aerosol. TEM images of air-dried Hg^O + I reaction products were collected from the gas-aerosol mixture. The size of the particles in the gas–aerosol

Fig. 7. MALDI-TOF mass spectrum of products formed in the reaction of Hg^0 with iodine oxide radicals

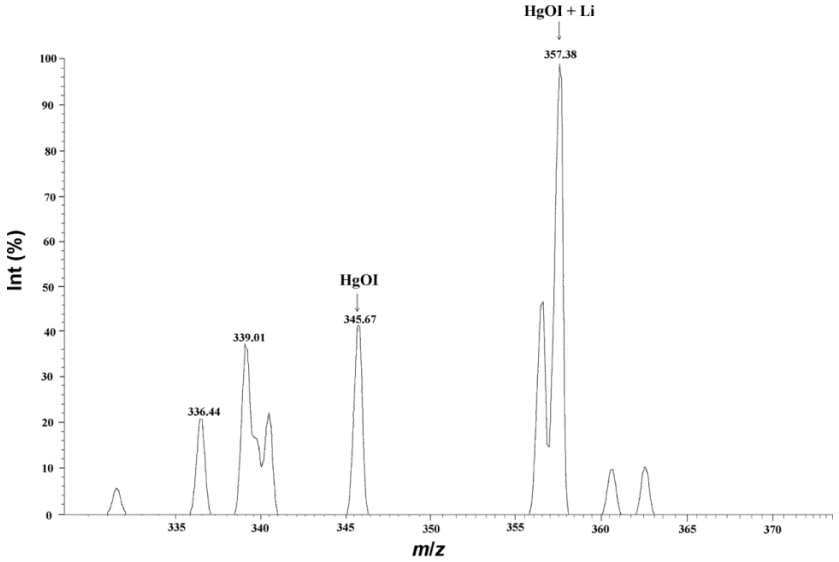

Fig. 8. (*a*) EDS spectrum shows the chemical composition of the product collected from the gas–aerosol in the reaction of Hg^0 with molecular iodine dispersed onto carbon-supported Cu grid. Inset shows HRTEM image of air-dried product collected from the gas–aerosol. (*b*) EDS spectrum shows the chemical composition of the product collected from the walls of the reaction chamber in the reaction of Hg^0 with molecular iodine dispersed onto carbon-supported Cu grid. Inset shows an HRTEM image of air-dried product collected from the walls of the reaction chamber.

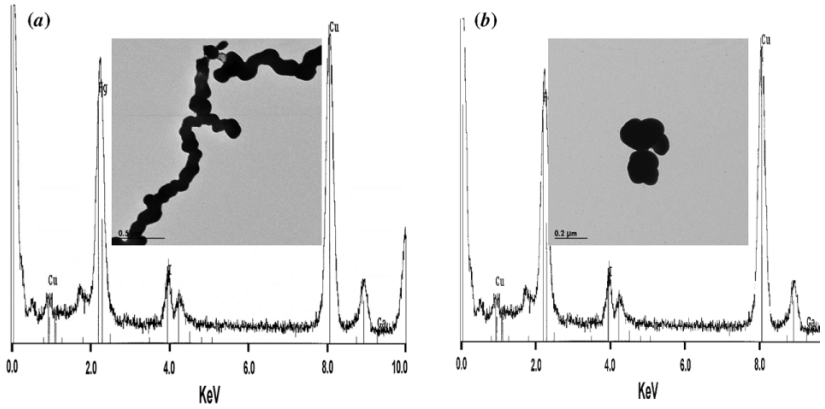

mixture was approximately 0.2 μm (Fig. 9*a*). The EDS spectrum of the chemical composition of the products in the gas–aerosol mixture showed that the gas–aerosol mixture contained mercury and iodine. Because of the chemical composition of the reaction products, we believe that the observed aerosol contains HgI_2. A TEM image of collected products of the reaction of $Hg^0 + I^{\cdot}$ from the walls of the reaction chamber is illustrated in Fig. 9*b*. The size and chemical composition of the particles collected from the walls of the reaction chamber exhibited similar features to those observed from gas–aerosol. Figure 10*a* illustrates the TEM image of air-dried products of the reaction of $Hg^0 + IO^{\cdot}$ that were collected from the gas–aerosol mixture. Particles in the gas–aerosol mixture were observed to be approximately 0.5 μm. The EDS spectrum of the chemical composition of the products in the gas–aerosol mixture revealed the presence of mercury, iodine, and oxygen. Because of the elemental composition of the reaction products, we believe that the observed aerosol contains Hg, O, and I. Collected products from the walls of the reaction chamber are found to have similar size and elemental composition to those observed from the gas–aerosol mixture (Fig. 10).

In the sixth method, we used CVAFS to quantify mercury products in the gas phase, aerosol, and as deposit on the walls of the reaction chamber. Upon completion of the reaction (confirmed by disappearance of MS peak due to Hg^0), the reaction flask was evacuated through a 0.45 μm Teflon filter to a residual pressure of ~0.0007 bar. The filter was treated with a HNO_3/H_2O_2 mixture. CVAFS analysis indicated that ~ (10 ± 1)% of total mercury (relative to the amount of Hg^0 loaded in the flask) was converted to mercury compounds in the aerosol phase. In another set of experiments, products were collected in a cooled coiled Pyrex trap, treated with the HNO_3/H_2O_2 mixture and further analyzed using CVAFS upon completion of the reaction. By subtracting the total mercury collected from the gas and aerosol mixtures and the amount of aerosol mercury collected on the filters, we obtained only ~ (10 ± 3)% of total mercury remaining in the gas phase. This analysis recovered (20 ± 4)% of the mercury in the gas–aerosol phase. Finally, the reaction

Fig. 9. (*a*) EDS spectrum shows the chemical composition of the product collected from the gas–aerosol in the reaction of Hg^0 with atomic iodine dispersed onto carbon-supported Cu grid. Inset shows an HRTEM image of air-dried product collected from the gas–aerosol. (*b*) EDS spectrum shows the chemical composition of the product collected from the walls of the reaction chamber in the reaction of Hg^0 with atomic iodine dispersed onto carbon-supported Cu grid. Inset shows an HRTEM image of air-dried product collected from the walls of the reaction chamber.

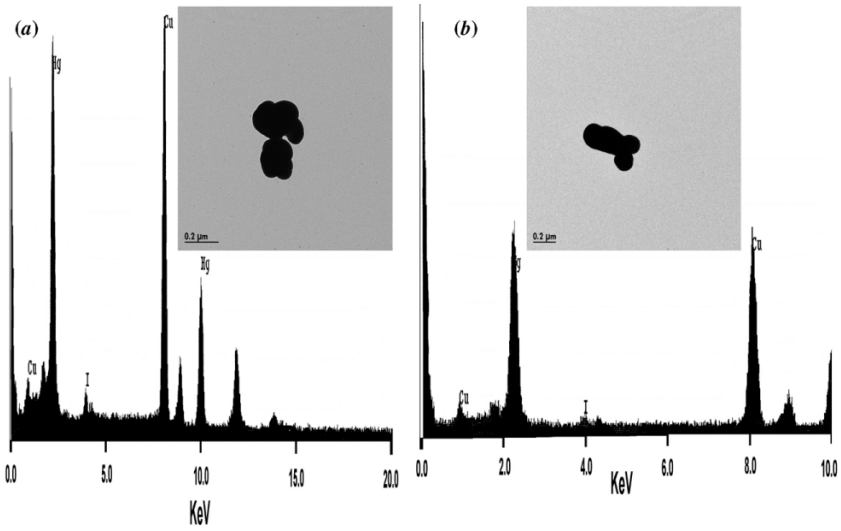

Fig. 10. (*a*) EDS spectrum shows the chemical composition of the product collected from the gas–aerosol in the reaction of Hg^0 with iodine oxide radicals dispersed onto carbon-supported Cu grid. Inset shows an HRTEM image of air-dried product collected from the gas–aerosol. (*b*) EDS spectrum shows the chemical composition of the product collected from the walls of the reaction chamber in the reaction of Hg^0 with iodine oxide radicals dispersed onto carbon-supported Cu grid. Inset shows an HRTEM image of air-dried product collected from the walls of the reaction chamber.

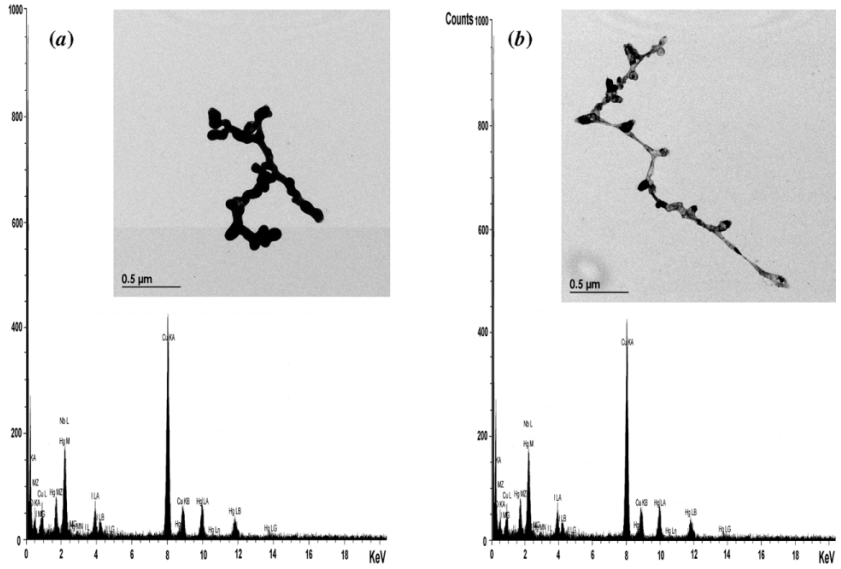

products were collected from the reaction flask walls by washing with a HNO_3/H_2O_2 mixture, and analyzed by CVAFS. Overall, (70 ± 5)% of Hg was recovered from the walls (Table 1). The dominant reaction products were found as adsorbed deposits on the walls of the reaction chamber (85 ± 2)% or as aerosols ~ (14 ± 1)% leaving only ~ (4 ± 1)% of the total mercury existing in the gas phase, as illustrated in Table 1.

As shown in Table 1 for [R5], ~ (25 ± 3)% of total mercury remains in the gas–aerosol phase with ~ (5 ± 2)% of total mercury recovered from the gas phase. Recovery of Hg from the walls of the reaction chamber was (75 ± 4)%. Our results therefore showed that the reaction products were predominantly found adsorbed on the walls of the reaction chamber as deposits or existed as aerosols. Under our experimental conditions, we did not observe any difference in identified mercury compounds in N_2 or air, noting that our nitrogen diluent (99.998%) gas was still not entirely oxygen free.

Potential reactions mechanism

Products of the oxidation of Hg^0 by I_2, I, and IO can be formed by reactions [R3] to [R5]

Table 1. Quantification of mercury in the reaction vessel for I_2-, I˙-, and IO˙-initiated reaction of gaseous mercury using a 0.45 μm Teflon filter.

	Mercury species								
	I_2			I			IO		
	Gas + aerosols	Aerosols	Wall deposits	Gas + aerosols	Aerosols	Wall deposits	Gas + aerosols	Aerosols	Wall deposits
Yield (%)	30±3	20±4	75±5	18±1	14±3	85±2	30±2	25±3	75±2
Char. Width (μm)	~0.2	~0.2	~0.5	~0.2	~0.2	~0.2	~0.5	~0.5	~0.5

[R1] $CH_2I_2 + h\upsilon\ (300 \leq \lambda \leq 400\ nm) \rightarrow CH_2I^{\cdot} + I^{\cdot}$

[R2] $I^{\cdot} + O_3 \rightarrow IO^{\cdot} + O_2$

[R3*a*] $Hg + I_2 \rightarrow HgI_2$

[R4*a*] $Hg + I^{\cdot} \rightarrow HgI$

[R4*b*] $HgI + I^{\cdot} \rightarrow HgI_2$

[R5*a*] $Hg + IO^{\cdot} \rightarrow HgOI/HgIO$

[R5*b*] $Hg + IO^{\cdot} \rightarrow HgO + I^{\cdot}$

[R5*c*] $Hg + IO^{\cdot} \rightarrow HgI + O$

[R5*d*] $HgI + IO^{\cdot} \rightarrow HgI_2 + O$

We identified HgI_2, HgIO or HgOI, HgO, and HgI by direct mass with a chemical ionization ion source. There are two possible sources for HgI, either as a product in the chamber or a fragmentation product of HgI_2 in the ion source of the mass spectrometer. Shepler et al. (48) have estimated the enthalpies of the above reaction at 0 K. This theoretical study used the ab initio CCSD(T) method with basis sets including detailed treatment of core–valence correlation, scalar reactivity, spin–orbit coupling, and the Lamb shift. The values of ΔH_r(0 K) for reactions [R5*a*–R5*d*] have been shown to be –51.2, 191.5, 209.2, and –28.6 kJ mol^{-1}, respectively. Regarding the results for ΔH_r(0 K), HgIO but not HgI and HgO cannot be formed by reactions [R5*b*] and [R5*c*], respectively. HgO can, however, be formed by reaction [R5*b*], and we did observe the existence of HgO with different types of mass spectrometry and HRTEM-EDS. The value of ΔH_r(0 K) = –146.4 kJ/mol for reaction [R3*a*] for the I_2-initiated reaction of gaseous mercury indicates this pathway is possible in the formation of HgI_2. We can indeed observe HgI_2, as confirmed by the different types of mass spectrometry technique used in this study.

Because we observed aerosols, and although we have modified the surface-to-volume ratios and the properties of the surfaces, and used different oxidant and reactant concentration regimes, we cannot rule out the possibility of heterogeneous reactions.

Summary and future work

We have studied the products of the reactions of gaseous mercury with molecular iodine, atomic iodine, and iodine oxide radicals at atmospheric pressure and room temperature in air and in N_2. For the first time, HgI_2, HgO, and HgOI/HgIO are identified as reaction products in the gas and in the aerosol phase, as well as on the walls of the reaction chamber. Our upper-limit rate constant for reaction of Hg^0 with molecular iodine is found to be $\leq (1.27 \pm 0.58) \times 10^{-19}$ cm^3 molecule^{-1} s^{-1}. It remains a possibility that during springtime in the Arctic and Antarctica, the iodine reactions have some significance. The reaction of molecular iodine is apparently too slow for the rapid depletion of elemental mercury in the boundary layer. We suspect that based on the formation rates of products in the course of I + Hg(0) reactions, the reactions of I are slower or at most comparable to the reactions of elemental mercury with Br (40, 49). However, the impact of iodine and iodine oxide in the production of oxidized mercury in atmospheric depletion should be further studied.

Acknowledgements

We would like to cordially thank Dr. Paterson for his valuable insights. We thank the Natural Sciences and Engineering Research Council of Canada (NSERC), Le Fonds québecois de la recherche sur la nature et les technologies (FQRNT), the Canadian Foundation for Innovation (CFI), the COMERN project, Canadian Foundation for Climate and Atmospheric Sciences (CFCAS), and Environment Canada for financial support. We would also like to thank Jackie Johnstone for proof reading the manuscript.

References

1. C.J. Lin and S.O. Pehkonen. Atmos. Environ. **33**, 2067 (1999).
2. S.M. Siegel and B.Z. Siegel. Nature (London, UK), **309**, 146 (1984).
3. Z.F. Xiao, J. Munthe, W.H. Schroeder, and O. Lindqvist. Tellus B. **43**, 267 (1991).
4. R.P. Mason, W.F. Fitzgerald, and F.M.M. Morel. Geochim. Cosmochim. Acta **58**, 3191 (1994).
5. S.E. Lindberg, K.H. Kim, T.P. Meyers, and J.G. Owens. Environ. Sci. Technol. **29**, 126 (1995).
6. N. Pirrone and K. Mahaffey. Dynamics of mercury pollution on regional and global scales. Springer. 2005.
7. R. Ferrara, B.E. Maserti, H. Edner, P. Ragnarson, S. Svanberg, and E. Wallinder. Atmos. Environ. Gen. Top. **26**, 1253 (1992).
8. N. Pirrone, G.J. Keeler, and J.O. Nriagu. Atmos. Environ. **30**, 2981 (1996).
9. A. Carpi and S.E. Lindberg. Environ. Sci. Technol. **31**, 2085 (1997).
10. L.D. Lacerda. Water Air Soil Pollut. **97**, 209 (1997).
11. J.T. Dvonch, J.R. Graney, G.J. Keeler, and R.K. Stevens. Environ. Sci. Technol. **33**, 4522 (1999).
12. F.J.G. Laurier, R.P. Mason, L. Whalin, and S. Kato. J. Geophys. Res. Atmos. **108** (2003).
13. W.H. Schroeder, K.G. Anlauf, L.A. Barrie, J.Y. Lu, A. Steffen, D.R. Schneeberger, and T. Berg. Nature (London, UK), **394**, 331 (1998).

14. J.Y. Lu, W.H. Schroeder, L.A. Barrie, A. Steffen, H.E. Welch, K. Martin, L. Lockhart, R.V. Hunt, G. Boila, and A. Richter. Geophys. Res. Lett. **28**, 3219 (2001).
15. S.E. Lindberg, S. Brooks, C.J. Lin, K.J. Scott, M.S. Landis, R.K. Stevens, M. Goodsite, and A. Richter. Environ. Sci. Technol. **36**, 1245 (2002).
16. L. Poissant and M. Pilote. J. Phys. IV. **107**, 1079 (2003).
17. L.A. Barrie, J.W. Bottenheim, R.C. Schnell, P.J. Crutzen, and R.A. Rasmussen. Nature (London, UK), **334**, 138 (1988).
18. B.J. Finlayson-Pitts, F.E. Livingston, and H.N. Berko. Nature (London, UK), **343**, 622 (1990).
19. K.L. Foster, R.A. Plastridge, J.W. Bottenheim, P.B. Shepson, B.J. Finlayson-Pitts, and C.W. Spicer. Science (Washington, DC), **291**, 471 (2001).
20. C.W. Spicer, R.A. Plastridge, K.L. Foster, B.J. Finlayson-Pitts, J.W. Bottenheim, A.M. Grannas, and P.B. Shepson. Atmos. Environ. **36**, 2721 (2002).
21. P.A. Ariya, A.P. Dastoor, M. Amyot, W.H. Schroeder, L. Barrie, K. Anlauf, F. Raofie, A. Ryzhkov, D. Davignon, J. Lalonde, and A. Steffen. Tellus B, **56**, 397 (2004).
22. S.E. Lindberg and W.J. Stratton. Environ. Sci. Technol. **32**, 49 (1998).
23. W.H. Schroeder, G. Yarwood, and H. Niki. Water Air Soil Pollut. **56**, 653 (1991).
24. B. Pal and P.A. Ariya. Phys. Chem. Chem. Phys. **6**, 572 (2004).
25. F. Raofie and P.A. Ariya. J. Phys. IV. **107**, 1119 (2003).
26. F. Raofie and P.A. Ariya. Environ. Sci. Technol. **38**, 4319 (2004).
27. B. Pal and P.A. Ariya. Environ. Sci. Technol. **38**, 5555 (2004).
28. P.A. Ariya, A. Khalizov, and A. Gidas. J. Phys. Chem. A, **106**, 7310 (2002).
29. A.F. Khalizov, B. Viswanathan, P. Larregaray, and P.A. Ariya. J. Phys. Chem. A, **107**, 6360 (2003).
30. A. Saiz-Lopez and J.M.C. Plane. Geophys. Res. Lett. **31** (2004).
31. J.E. Lovelock and R.J. Maggs. Nature (London, UK), **241**, 194 (1973).
32. J.A. Garland and H. Curtis. J. Geophys. Res. Oceans Atmos. **86**, 3183 (1981).
33. D. Davis, J. Crawford, S. Liu, S. McKeen, A. Bandy, D. Thornton, F. Rowland, and D. Blake. J. Geophys. Res. Atmos. **101**, 2135 (1996).
34. L.J. Carpenter, W.T. Sturges, S.A. Penkett, P.S. Liss, B. Alicke, K. Hebestreit, and U. Platt. J. Geophys. Res. Atmos. **104**, 1679 (1999).
35. B. Alicke, K. Hebestreit, J. Stutz, and U. Platt. Nature (London, UK), **397**, 572 (1999).
36. B.J. Allan, G. McFiggans, J.M.C. Plane, and H. Coe. J. Geophys. Res. Atmos. **105**, 14363 (2000).
37. G. McFiggans, R.A. Cox, J.C. Mossinger, B.J. Allan, and J.M.C. Plane. J. Geophys. Res. Atmos. **107** (2002).
38. S. Solomon, R.R. Garcia, and A.R. Ravishankara. J. Geophys. Res. Atmos. **99**, 20491 (1994).
39. Y. Nakano, S. Enami, S. Nakamichi, S. Aloisio, S. Hashimoto, and M. Kawasaki. J. Phys. Chem. A, **107**, 6381 (2003).
40. J.G. Calvert and S.E. Lindberg. Atmos. Environ. **38**, 5105 (2004).
41. S. Coquet and P.A. Ariya. Int. J. Chem. Kinet. **32**, 478 (2000).
42. M.E. Jenkin, R.A. Cox, and D.E. Candeland. J. Atmos. Chem. **2**, 359 (1985).
43. G. Snider, F. Raofie, and P.A. Ariya. Phys. Chem. Chem. Phys. In press. (2008).
44. E. Bulska, H. Emteborg, D.C. Baxter, W. Frech, D. Ellingsen, and Y. Thomassen. Analyst, **117**, 657 (1992).
45. J. Snell, J. Qian, M. Johansson, K. Smit, and W. Frech. Analyst, **123**, 905 (1998).
46. M. Karas and R. Kruger. Chem. Rev. **103**, 427 (2003).
47. F. Raofie and P.A. Ariya. American Geophysical Union, Spring Meeting, San Francisco, CA, USA. 2006.
48. B.C. Shepler, N.B. Balabanov, and K.A. Peterson. J. Phys. Chem. A, **109**, 10363 (2005).
49. D.L. Donohoue, D. Bauer, B. Cossairt, and A.J. Hynes. J. Phys. Chem. A, **110**, 6623 (2006).